International Journal of Engineering Research & Technology (IJERT)
ISSN: 2278-0181
Vol. 15 Issue 10 , October - 2026

Performance Evaluation of Coconut Fibre as a Sustainable Additive in Water-Based Drilling Fluid

Igoru Ufuoma Alex
Department of Petroleum Engineering, Faculty of Engineering, Delta State University, Abraka, Nigeria
Corresponding author: ufuomaigoru@delsu.edu.ng
ORCID: https://orcid.org/0009-0002-7161-4459

Abstract - Water-based drilling fluids require appropriate rheological and filtration properties to ensure effective cuttings transport, wellbore stability and reduced filtrate invasion. This study evaluated coconut fibre (CF), sourced locally, as a biodegradable additive in bentonite–barite water-based drilling mud. Three formulations comprising a base mud and modified muds containing 12.5 g and 25.0 g CF per 250 mL of base mud were prepared. CF was characterised using X-ray diffraction (XRD) and Fourier-transform infrared (FTIR) spectroscopy. Mud density, pH, plastic viscosity (PV), apparent viscosity (AV), yield point (YP), gel strength, API filtrate loss and filter-cake thickness were evaluated before and after ageing at 65 °C for 16hours. XRD revealed a broad diffraction maximum at 2θ = 21.36 ± 0.06°, indicating predominantly amorphous /low-crystallinity material, while FTIR confirmed characteristic functional groups associated with a cellulose–lignin matrix. Increasing CF concentration enhanced PV, AV, YP and gel strength while reducing mud density and pH. Compared with the base mud, the 12.5 g formulation reduced API filtrate loss from 22.5 to 18.0 mL (20.00%) and filter-cake thickness from 2.10 to 1.70 mm (19.05%). The 25.0 g formulation achieved greater reductions of 35.56% and 38.10%, respectively. Following ageing, the CF-modified muds maintained lower filtrate loss than the base mud, recording 15.0 mL compared with 24.0 mL. These findings demonstrate the potential of coconut fibre as a locally available biodegradable additive for improving filtration control and modifying drilling fluid rheology. Further optimisation is required to establish its suitability under field conditions.

Keywords: coconut fibre; water-based drilling fluid; drilling mud; rheology; fluid loss; filter cake; X-ray diffraction; FTIR; Agricultural waste.

1. INTRODUCTION

Drilling fluids are engineered systems circulated through a wellbore to transport drilled cuttings, control formation pressure, cool and lubricate the bit and drill string, maintain wellbore stability and reduce formation damage. Their performance depends on density, rheology, filtration behaviour, gel strength, pH, solids concentration and chemical compatibility with the formation and other mud constituents **[1]; [2]**. In water-based muds, PV, AV, YP and gel strength govern resistance to flow and the capacity of the mud to suspend and transport cuttings under circulating and static conditions. Filtration control is equally important because excessive filtrate invasion can alter near-wellbore properties, contribute to formation damage and destabilize sensitive formations. **[3].** Fluid-loss-control materials promote the development of a low-

(This work is licensed under a Creative Commons Attribution 4.0 International License.)

International Journal of Engineering Research & Technology (IJERT)
ISSN: 2278-0181
Vol. 15 Issue 10 , October - 2026

permeability filter cake that restricts continued filtrate invasion **[4]; [2].** Conventional systems commonly use cellulose derivatives, starches, xanthan and other polymers. Renewable biomass-derived materials are increasingly investigated because they can provide functional polysaccharides, fibres and mineral constituents while potentially reducing dependence on petroleum-derived or highly processed additives **[5]; [6].**

Coconut fibre is particularly attractive because coconut processing produces substantial lignocellulosic residue. Coconut coir contains a lignin-rich matrix and structural polysaccharides that can provide a fibrous framework in composite materials [7]. Recent drilling-fluid studies have reported that coconut-derived materials can influence rheology and filtration, with particle size, concentration and temperature affecting performance **[8]; [9].** A recent study of burnt coconut fibre likewise reported measurable effects on rheology, filtration and pH in water-based muds **[10].** The behaviour of a biomass additive in a clay-based mud depends on its physical structure and surface chemistry. FTIR can identify functional groups associated with cellulose, hemicellulose and lignin, while XRD can provide information on the degree of structural order in cellulose-containing materials **[7]; [11].** These characteristics are relevant because hydration, hydrogen bonding, particle interaction and pore bridging can influence both rheology and filter-cake development **[2]; [6].** This study characterises coconut fibre using XRD and FTIR and evaluates its influence on density, pH, rheology, gel strength, API filtration loss and filter-cake thickness at two loadings. The effect of thermal ageing at 65 °C for 16 h is also examined. The study is deliberately interpreted within the laboratory conditions used and does not claim field suitability.

2. MATERIALS AND METHODS

2.1 Materials

Sodium bentonite served as the primary viscosifier, barite as the weighting agent and distilled water as the continuous phase **[11]**. Coconut fibre was used as the test additive. **[8].** The materials and their sources are listed in Table 1.

Table 1. Materials, sources and functions.

Material	Source / supplier	Function
Sodium bentonite	Drilling Laboratory, Department of Petroleum and Gas Engineering, Delta State University, Oleh Campus; commercial drilling-grade sodium bentonite	Primary viscosifier
Barite	Drilling Laboratory, Department of Petroleum and Gas Engineering, Delta State University, Oleh Campus; commercial drilling-grade barite	Weighting agent

(This work is licensed under a Creative Commons Attribution 4.0 International License.)

International Journal of Engineering Research & Technology (IJERT)
ISSN: 2278-0181
Vol. 15 Issue 10 , October - 2026

Distilled water	Drilling Laboratory, Department of Petroleum and Gas Engineering, Delta State University, Oleh Campus; laboratory-prepared distilled water	Continuous phase
Coconut fibre (CF)	Ozoro Main Market, Isoko North LGA, Delta State, Nigeria	Test additive

2.2 Preparation of Coconut Fibre

Coconut fibre was manually cleaned to remove dirt and foreign matter, washed and repeatedly rinsed with distilled water, and oven-dried at 70 °C for 4 h. The dried fibre was ground using an electric laboratory grinding mill and passed through a 10 µm sieve to obtain a relatively uniform fine material. Washing, drying, grinding and sieving are commonly used in lignocellulosic biomass processing to remove surface impurities, reduce particle size and improve material uniformity before subsequent characterisation **Moraes *et al*., (2024**); **[13].** The prepared fibre was stored in a clean, dry container until use to minimise contamination and moisture uptake before experimentation.

2.3 Characterisation of Coconut Fibre

X-ray diffraction (XRD) and Fourier-transform infrared spectroscopy (FTIR) were used to characterise the structural and functional-group features of the prepared coconut fibre. XRD provides information about crystalline structure and diffraction-peak characteristics, whereas FTIR identifies characteristic vibrational bands associated with chemical bonds and functional groups in lignocellulosic materials **[14]; [13].** These complementary techniques are useful for investigating the structural and chemical characteristics of coconut-derived materials.

2.3.1 X-ray diffraction

X-ray diffraction (XRD) patterns were recorded using Cu Kα radiation (\(\lambda = 1.5406\) Å) over a \(2\theta\) range of 3–70°, with a step size of 0.02° and a counting time of 1 s per step. The instrument was operated with a fixed divergence slit of 1°, a receiving slit of 0.1 mm, a goniometer radius of 240 mm, no incident-beam monochromator and no sample spinning. The powdered fibre was mounted on the sample holder before measurement. These instrument settings describe the experimental conditions used in this study and should be verified against the instrument's acquisition file. The principal broad diffraction maximum was profile-fitted using a split pseudo-Voigt function. The fitted parameters included peak position, interplanar spacing (\(d\)-spacing), peak height, full width at half maximum (FWHM), integral width and integrated intensity. The interplanar spacing was determined using Bragg's law, while the apparent crystallite size may be estimated from diffraction-peak broadening using the Scherrer equation, provided

(This work is licensed under a Creative Commons Attribution 4.0 International License.)

International Journal of Engineering Research & Technology (IJERT)
ISSN: 2278-0181
Vol. 15 Issue 10 , October - 2026

that instrumental broadening is accounted for where appropriate **[15]; [14].** These parameters help describe the diffraction profile and the crystalline features of lignocellulosic materials, although the apparent crystallite size should not be interpreted as the overall fibre particle size. The apparent crystallite size is treated only as a descriptive peak-broadening parameter because the pattern is dominated by diffuse scattering. Cellulose I commonly shows principal reflections near 2θ = 14.8°, 16.5° and 22.5° **[16].**

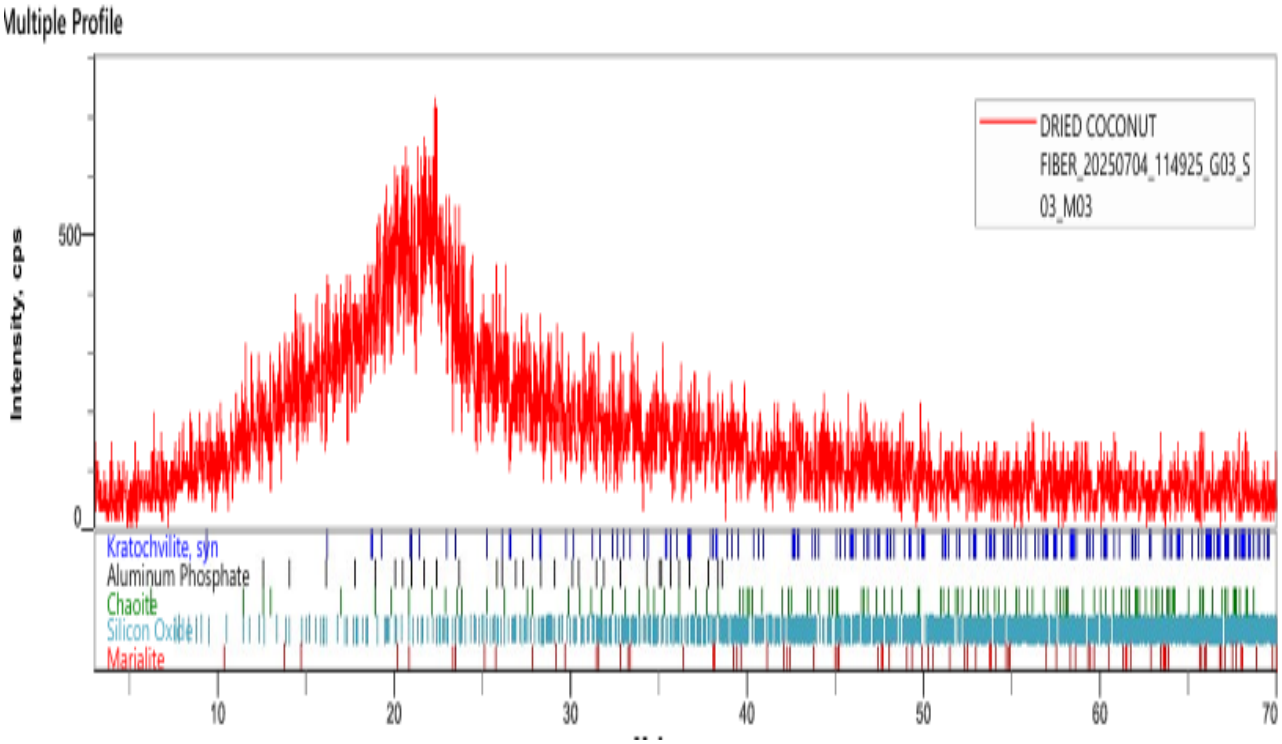


Figure 1. (a) XRD pattern of coconut fibre over 2θ = 3–70°, showing the broad principal diffraction maximum centred near 21.36°.

(This work is licensed under a Creative Commons Attribution 4.0 International License.)

International Journal of Engineering Research & Technology (IJERT)
ISSN: 2278-0181
Vol. 15 Issue 10 , October - 2026

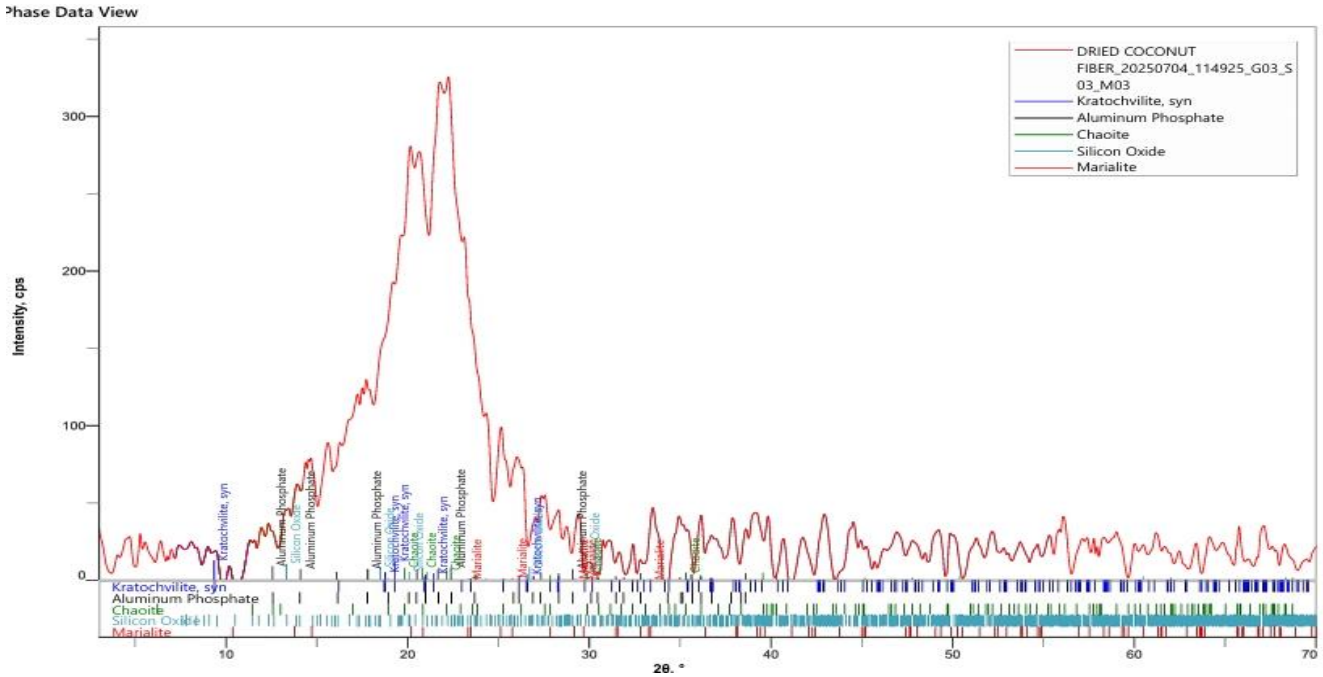


Figure 1 (b) smoothed pattern with the reference lines of the candidate phases returned by the search–match.

Table 2. Profile-fitted parameters of the principal XRD maximum of coconut fibre.

Parameter	**CF**
2θ (°)	21.36 ± 0.06
d-spacing (Å)	4.156 ± 0.012
Height (cps)	159 ± 30
FWHM (°)	6.66 ± 0.06
Integral width (°)	7.3 ± 1.5
Integrated intensity (cps·°)	1167 ± 16
Apparent crystallite size (Å)	12.69 ± 0.11
Profile asymmetry	1.44 ± 0.06

The profile is dominated by one broad, asymmetric maximum with no resolved sharp crystalline reflections. Although its position is close to the main cellulose I reflection, the strong broadening and absence of the other characteristic reflections indicate that the material is predominantly amorphous or of very low apparent crystallinity. Automated phase-search results from the source analysis produced low-confidence candidate matches, but these were not treated as evidence of crystalline phases because the candidates are not

(This work is licensed under a Creative Commons Attribution 4.0 International License.)

International Journal of Engineering Research & Technology (IJERT)
ISSN: 2278-0181
Vol. 15 Issue 10 , October - 2026

supported by resolved diffraction peaks. No crystallinity index was calculated because the raw intensity values required for a defensible Segal calculation were not available as a complete numerical dataset.

2.3.2 Fourier-transform infrared spectroscopy

FTIR spectra were recorded in attenuated total reflectance mode over 4000–400 cm^{-1} at a resolution of 4 cm^{-1}. The principal observed bands were assigned using standard group-frequency information **[17]** and interpreted in relation to the known lignocellulosic structure of coconut coir **[7].**

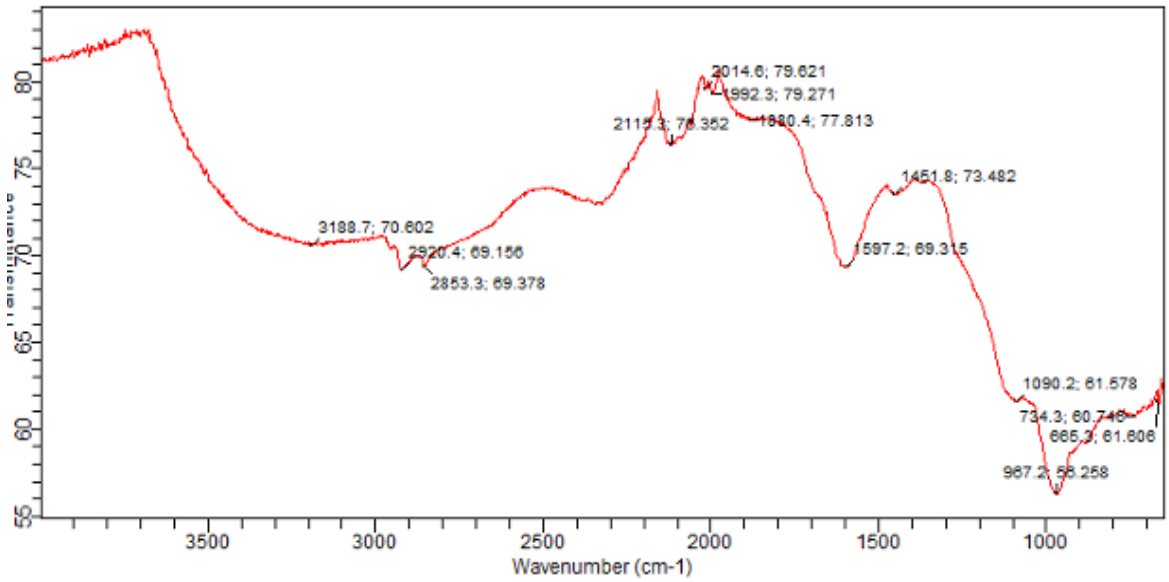


Figure 2. FTIR spectrum of coconut fibre over 4000–400 cm^{-1} with the principal observed bands.

Table 3. Principal FTIR bands and assignments for coconut fibre.

Observed wavenumber (cm^{-1})	Assignment	Likely component
3188.7	O–H stretching, hydrogen-bonded	Cellulose, hemicellulose and lignin
2920.4	Asymmetric aliphatic C–H stretching	Cellulose, hemicellulose and lignin
2853.3	Symmetric aliphatic C–H stretching	Cellulose, hemicellulose and lignin
1597.2	Aromatic C=C stretching	Lignin
1451.8	C–H bending / aromatic skeletal vibration	Lignin and cellulose
1090.2	C–O / C–O–C stretching	Cellulose and hemicellulose
967.2	Fingerprint-region C–O/C–H vibration	Polysaccharide matrix
734.3, 665.3	Fingerprint-region C–H out-of-plane bending	Aromatic/polysaccharide matrix

(This work is licensed under a Creative Commons Attribution 4.0 International License.)

International Journal of Engineering Research & Technology (IJERT)
ISSN: 2278-0181
Vol. 15 Issue 10 , October - 2026

The broad O–H band at 3188.7 cm^{-1} indicates hydrogen-bonded hydroxyl groups, while the 2920.4 and 2853.3 cm^{-1} bands correspond to aliphatic C–H stretching. The 1597.2 cm^{-1} band is consistent with aromatic lignin structures, and the 1090.2 cm^{-1} band is associated with C–O/C–O–C stretching in polysaccharide structures. Together, the spectrum is consistent with a cellulose–lignin-rich lignocellulosic material **[7]; [17].**

2.4 Preparation of Drilling Mud Samples

The base mud consisted of 250 mL distilled water, 15.5 g sodium bentonite and 75.0 g barite. Bentonite was added gradually to the water under continuous agitation and mixed at 2400 rpm for 20 min to promote hydration. Barite was then added gradually and mixed at 2400 rpm for a further 30 min until a visually homogeneous mud was obtained. Two modified mud samples were prepared by adding 12.5 and 25.0 g CF per 250 mL of base mud, equivalent to 5 and 10 g/100 mL, respectively. The fibre was added gradually under continuous agitation and mixed for a further 20 min at 2400 rpm. The same sequence and mixing conditions were used for all samples.

Table 4. Composition of the base and CF-modified mud samples.

Sample	Water (mL)	Bentonite (g)	Barite (g)	CF (g)	CF loading (g/100 mL)
Base Mud	250	15.5	75.0	0	0
CF-1	250	15.5	75.0	12.5	5
CF-2	250	15.5	75.0	25.0	10

2.5 Drilling-Mud Testing

Testing followed API RP 13B-1 procedures applicable to water-based drilling **[18]**. Mud density was measured using a calibrated mud balance and reported in lb/gal (ppg). pH was measured using a calibrated digital pH meter, with the electrode rinsed with distilled water before and after measurement. Rheological properties were measured at 25 °C (77 °F) using a Fann Model 35A rotational viscometer. Dial readings were recorded at 600, 300, 200, 100, 6 and 3 rpm in descending order after stabilisation. Ten-second and 10-min gel strengths were measured after the corresponding static periods.

Plastic viscosity, yield point and apparent viscosity were calculated from the 600- and 300-rpm dial readings as follows:

$$PV = \theta_{600} - \theta_{300} \text{ ----------(1)}$$

$$YP = \theta_{300} - PV \text{ ----------(2)}$$

(This work is licensed under a Creative Commons Attribution 4.0 International License.)

International Journal of Engineering Research & Technology (IJERT)
ISSN: 2278-0181
Vol. 15 Issue 10 , October - 2026

$$AV = \frac{\theta_{600}}{2} \text{ ---------- (3)}$$

where θ_{600} and θ_{300} are the dial readings at 600 and 300 rpm. PV and AV are reported in cP (mPa·s), while YP is reported in lb/100 ft². Filtration was evaluated using a low-pressure, low-temperature filter press at 100 psi for 30 min. Filtrate volume was recorded in millilitres and the resulting filter cake was removed carefully and measured with a digital Vernier caliper with 0.01 mm resolution.

2.6 Ageing of the Mud Samples

Aliquots of each mud sample were aged at 65 °C for 16 h in hot-rolling cells. After ageing, the samples were cooled to the test temperature, remixed for 25 min and re-tested for pH, rheological properties, gel strength and filtration behaviour. Aged results were compared descriptively with the corresponding unaged values.

2.7 Data Treatment

Measurements were performed in triplicate and are reported as mean ± standard deviation. Percentage changes were calculated descriptively relative to the base mud using:

$$\%\ change = \left[\frac{(X_t - (X_c)}{X_c}\right] \times 100 \text{ ----------(4)}$$

where X_t is the value for a treated mud and X□ is the value for the base mud. For filtrate loss and cake thickness, negative values indicate reductions relative to the base mud. No inferential statistical test or statistical software was used.

3. RESULTS AND DISCUSSION

3.1 Characterisation of Coconut Fibre

3.1.1 X-ray diffraction

The XRD pattern of CF is characterised by a broad, asymmetric maximum centred at 2θ = 21.36 ± 0.06° with d = 4.156 ± 0.012 Å and FWHM = 6.66 ± 0.06° (Figure 1; Table 2). No sharp, well-resolved crystalline reflections are visible across the scan. The maximum lies near the principal diffraction region of cellulose I, but its strong broadening and the absence of clearly resolved companion reflections indicate a highly disordered or very low-crystallinity structure rather than a well-developed cellulose crystal lattice **[16]**. The apparent crystallite-size value of 12.69 ± 0.11 Å should therefore be regarded as a peak-broadening descriptor rather than a direct measurement of a discrete crystallite population. The XRD interpretation is consistent with the lignocellulosic nature of coconut coir, in which cellulose is embedded in a matrix containing lignin and hemicellulosic components **[7].** The lack of convincing crystalline mineral peaks also means that the automated candidate-phase matches observed in the original analysis should not be used to

(This work is licensed under a Creative Commons Attribution 4.0 International License.)

International Journal of Engineering Research & Technology (IJERT)
ISSN: 2278-0181
Vol. 15 Issue 10 , October - 2026

claim specific inorganic phases. This conservative interpretation avoids assigning physically implausible crystalline compositions to a broad amorphous scattering profile.

3.1.2 Fourier-transform infrared spectroscopy

The FTIR spectrum (Figure 2; Table 3) confirms the presence of hydroxyl, aliphatic hydrocarbon, aromatic and polysaccharide-related functional groups. The broad O–H band at 3188.7 cm^{-1} is consistent with hydrogen-bonded hydroxyl groups in cellulose, hemicellulose and lignin. Bands at 2920.4 and 2853.3 cm^{-1} correspond to aliphatic C–H stretching, while the 1597.2 cm^{-1} band is associated with aromatic C=C vibration in lignin. The strong band near 1090.2 cm^{-1} is consistent with C–O/C–O–C stretching in polysaccharide structures **[17].** These features support the interpretation of CF as a cellulose–lignin-rich lignocellulosic material.

3.2 Density and pH

The base mud had a density of 11.50 ± 0.10 ppg, whereas CF-1 and CF-2 had densities of 8.80 ± 0.10 and 8.60 ± 0.10 ppg, respectively (Table 5; Figure 5). Thus, CF addition reduced density by 23.48% at 12.5 g loading and 25.22% at 25.0 g loading relative to the base mud. The reduction is expected because the added fibrous biomass replaces part of the volume fraction occupied by the denser barite-weighted mud without adding a high-density weighting material. From a drilling perspective, this density reduction is important because mud weight must remain sufficient to balance formation pressure; therefore, CF cannot be considered a direct substitute for barite.

The pH decreased from 8.40 ± 0.10 for the base mud to 7.50 ± 0.20 for CF-1 and 7.45 ± 0.00 for CF-2, corresponding to reductions of 10.71% and 11.31%, respectively. The change may reflect soluble components released from the fibre or changes in the aqueous phase, although soluble-ion composition was not measured. The measured pH values remained mildly alkaline, but the observed shift demonstrates that biomass addition can alter mud chemistry and should be considered during formulation.

Table 5. Density and pH of the unaged mud samples.

Sample	Density (ppg)	pH	Density change (%)	pH change (%)
Base Mud	11.50 ± 0.10	8.40 ± 0.10	0.00	0.00
CF-1	8.80 ± 0.10	7.50 ± 0.20	−23.48	−10.71

(This work is licensed under a Creative Commons Attribution 4.0 International License.)

International Journal of Engineering Research & Technology (IJERT)
ISSN: 2278-0181
Vol. 15 Issue 10 , October - 2026

CF-2	8.60 ± 0.10	7.45 ± 0.00	−25.22	−11.31

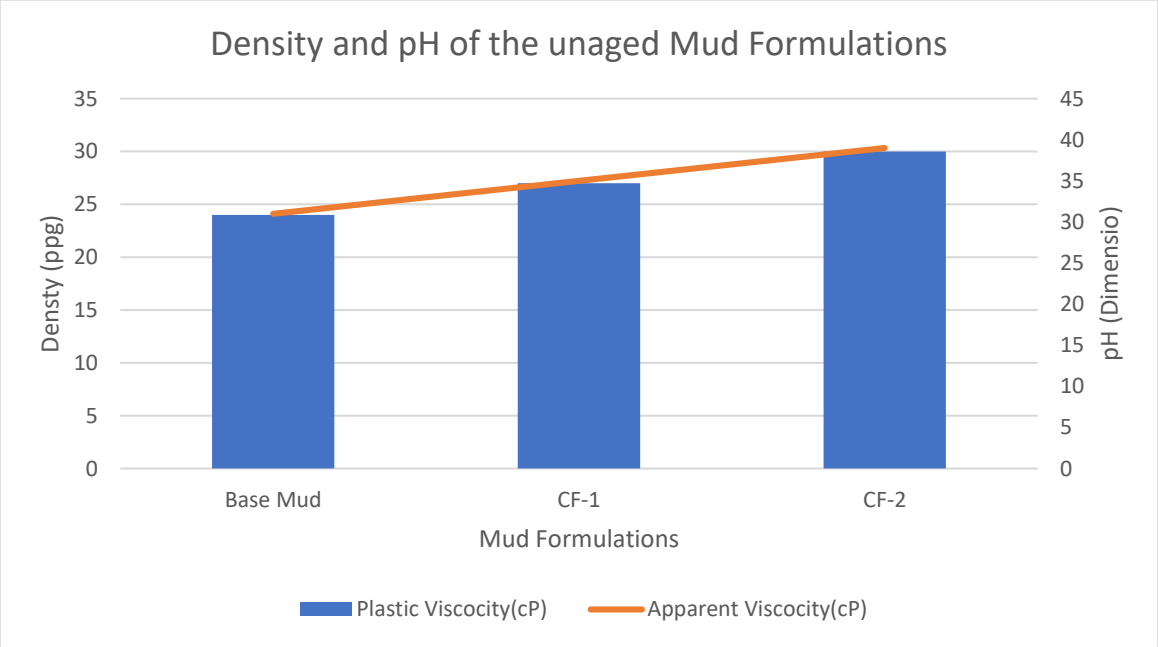


Figure 5. Density and pH of the unaged mud formulations.

3.3 Rheological Properties

CF increased all three principal rheological parameters. PV increased from 24.0 ± 1.0 cP in the base mud to 27.0 ± 1.0 cP in CF-1 and 30.0 ± 1.0 cP in CF-2, corresponding to increases of 12.50% and 25.00%, respectively. AV increased from 31.0 ± 0.5 to 35.0 ± 0.5 cP and 39.0 ± 0.5 cP, while YP increased from 14.0 ± 1.4 to 16.0 ± 1.4 and 18.0 ± 1.4 lb/100 ft². These progressive changes indicate that increasing CF loading increased the resistance of the mud to flow and strengthened particle–particle interactions. The increase in PV is consistent with the introduction of additional suspended fibrous solids and increased hydrodynamic interaction among fibre particles, bentonite platelets and the aqueous phase. The rise in YP suggests stronger low-shear structure, which can assist cuttings suspension and transport, although excessive viscosity can increase circulating pressure and equivalent circulating density. Similar concentration-dependent effects have been reported for coconut-derived and other biomass additives in water-based muds **[8]; [5].**

Table 6. Viscometer readings and calculated rheological properties of the unaged mud samples.

Sample	θ600	θ300	θ200	θ100	θ6	θ3	PV (cP)	AV (cP)	YP (lb/100 ft²)

(This work is licensed under a Creative Commons Attribution 4.0 International License.)

International Journal of Engineering Research & Technology (IJERT)
ISSN: 2278-0181
Vol. 15 Issue 10 , October - 2026

Base Mud	62.0 ± 1.0	38.0 ± 1.0	29.0 ± 1.0	20.0 ± 1.0	6.0 ± 0.6	4.0 ± 0.5	24.0 ± 1.4	31.0 ± 0.5	14.0 ± 1.4
CF-1	70.0 ± 1.0	43.0 ± 1.0	33.0 ± 1.0	23.0 ± 1.0	7.0 ± 0.6	5.0 ± 0.5	27.0 ± 1.4	35.0 ± 0.5	16.0 ± 1.4
CF-2	78.0 ± 1.0	48.0 ± 1.0	37.0 ± 1.0	26.0 ± 1.0	8.0 ± 0.6	6.0 ± 0.5	30.0 ± 1.4	39.0 ± 0.5	18.0 ± 1.4

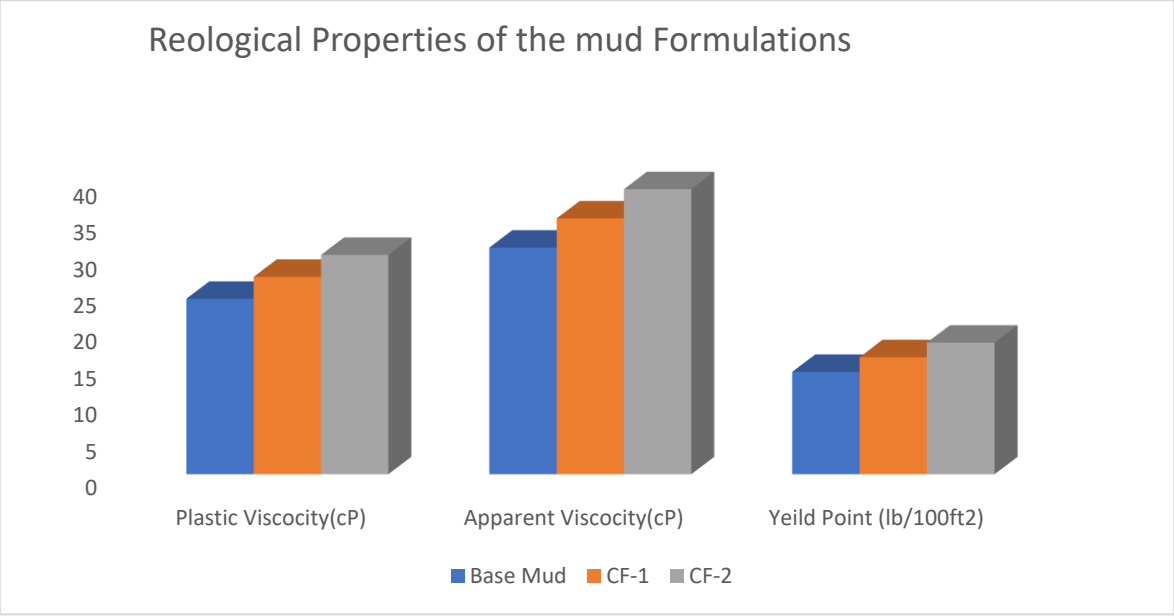


Figure 6. Plastic viscosity, apparent viscosity and yield point of the unaged mud formulations.

3.4 Gel Strength

The base mud exhibited 10-s and 10-min gel strengths of 6.0 ± 0.6 and 10.0 ± 1.0 lb/100 ft², respectively (Table 7; Figure 7). CF-1 increased these values to 8.0 ± 0.6 and 13.0 ± 1.0 lb/100 ft², while CF-2 increased them to 10.0 ± 1.0 and 16.0 ± 1.0 lb/100 ft². The increases were therefore progressive with loading. The 10-min gel was higher than the 10-s gel in every sample, showing progressive structure development during static ageing. This behaviour is consistent with the contribution of additional suspended particles and fibrous surfaces to the bentonite network. Adequate gel strength supports solids suspension when circulation stops, but excessive gel strength can increase the pressure required to restart circulation **[1].**

Table 7. Gel strengths of the unaged mud samples.

Sample	**10-s gel (lb/100 ft²)**	**10-min gel (lb/100 ft²)**	**10-s change (%)**	**10-min change (%)**
Base Mud	6.0 ± 0.6	10.0 ± 1.0	0.00	0.00
CF-1	8.0 ± 0.6	13.0 ± 1.0	33.33	30.00

(This work is licensed under a Creative Commons Attribution 4.0 International License.)

International Journal of Engineering Research & Technology (IJERT)
ISSN: 2278-0181
Vol. 15 Issue 10 , October - 2026

CF-2	10.0 ± 1.0	16.0 ± 1.0	66.67	60.00

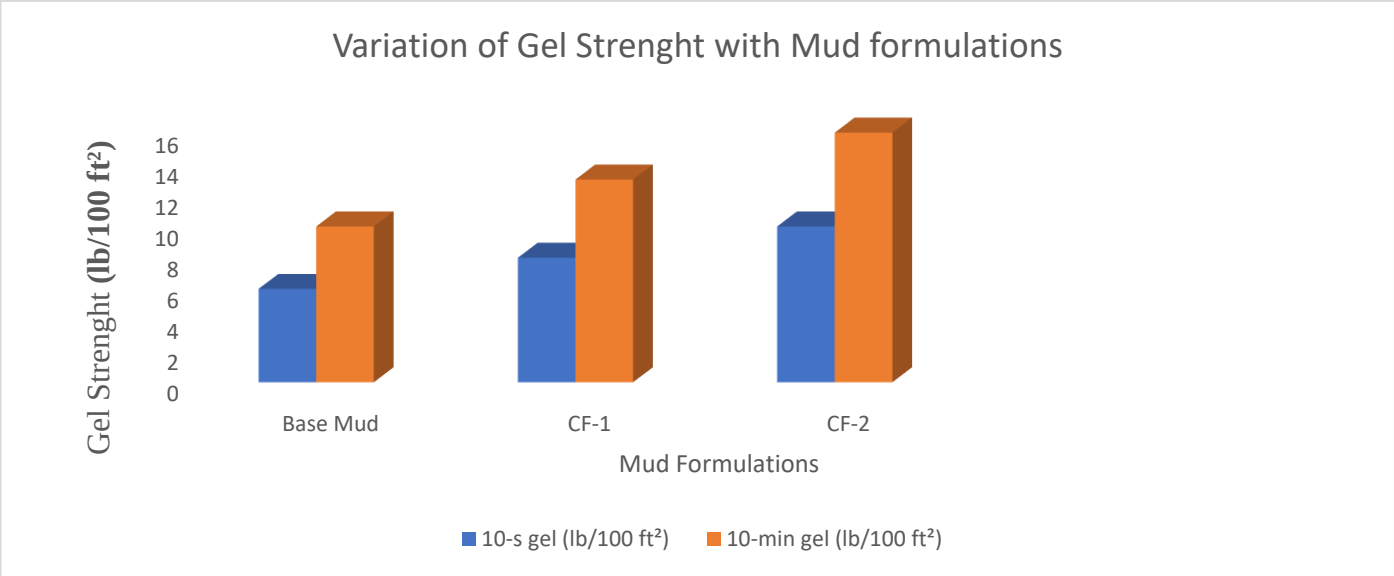


Figure 7. Ten-second and 10-min gel strengths of the mud formulations.

3.5 Filtration Behaviour and Filter-Cake Thickness

CF produced a clear improvement in filtration control. The base mud generated 22.5 ± 0.5 mL filtrate after 30 min, compared with 18.0 ± 0.4 mL for CF-1 and 14.5 ± 0.5 mL for CF-2 (Table 8; Figure 8). Relative to the base mud, these represent reductions of 20.00% and 35.56%, respectively. Filter-cake thickness also decreased from 2.10 ± 0.10 mm for the base mud to 1.70 ± 0.10 mm for CF-1 and 1.30 ± 0.10 mm for CF-2, corresponding to reductions of 19.05% and 38.10%. The simultaneous reduction in filtrate volume and cake thickness indicates that CF did not simply produce a thicker barrier; instead, the fibrous particles appear to have contributed to a more effective sealing structure. A plausible mechanism is that the fibres bridge larger pore openings while bentonite particles occupy smaller voids, reducing the permeability of the cake. This interpretation agrees with recent studies reporting concentration-dependent filtration control by coconut-derived fibres and other biodegradable materials **[8]; [9]; [5]**. The strongest filtration response occurred at the higher loading, indicating that the amount of available fibre was important under the conditions tested.

Table 8. API filtrate loss and filter-cake thickness of the unaged mud samples.

Sample	**Filtrate at 30 min (mL)**	**Cake thickness (mm)**	**Fluid-loss change (%)**	**Cake change (%)**
Base Mud	22.5 ± 0.5	2.10 ± 0.10	0.00	0.00

(This work is licensed under a Creative Commons Attribution 4.0 International License.)

International Journal of Engineering Research & Technology (IJERT)
ISSN: 2278-0181
Vol. 15 Issue 10 , October - 2026

CF-1	18.0 ± 0.4	1.70 ± 0.10	−20.00	−19.05
CF-2	14.5 ± 0.5	1.30 ± 0.10	−35.56	−38.10

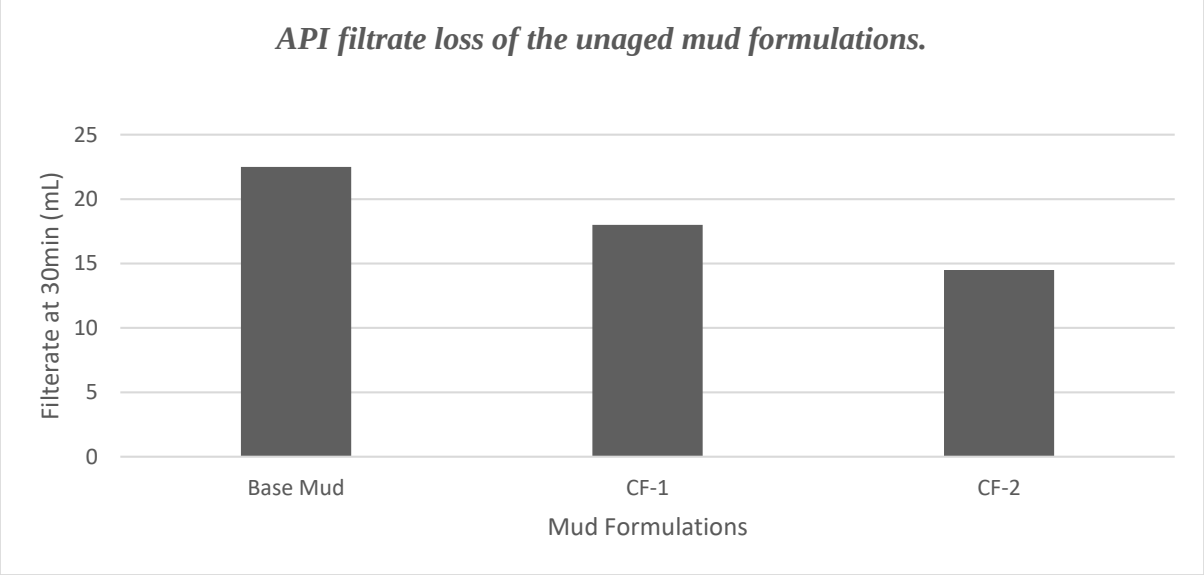


Figure 8. API filtrate loss of the unaged mud formulations.

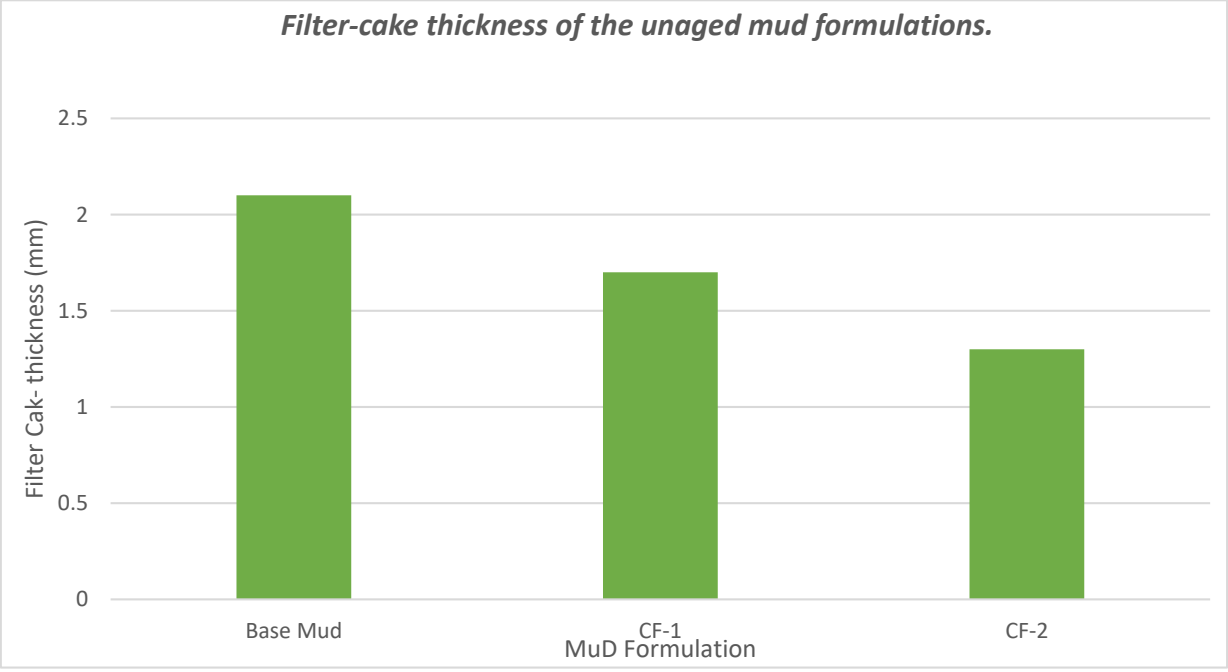


Figure 9. Filter-cake thickness of the unaged mud formulations.

3.6 Effect of Thermal Ageing

(This work is licensed under a Creative Commons Attribution 4.0 International License.)

International Journal of Engineering Research & Technology (IJERT)
ISSN: 2278-0181
Vol. 15 Issue 10 , October - 2026

Ageing at 65 °C for 16 h increased PV, AV and YP in all samples as shown in Table 9. For the base mud, PV increased from 24.0 to 27.0 cP (+12.50%), while CF-1 and CF-2 increased from 27.0 to 30.0 cP (+11.11%) and from 30.0 to 34.0 cP (+13.33%), respectively. YP increased by 57.14% in the base mud, 50.00% in CF-1 and 44.44% in CF-2. The smaller relative YP increase in CF-2 suggests that its stronger unaged structure did not undergo as large a proportional change during ageing as the base mud. Filtration performance was largely retained. Filtrate loss increased from 22.5 to 24.0 mL in the base mud (+6.67%), from 18.0 to 18.5 mL in CF-1 (+2.78%) and from 14.5 to 15.0 mL in CF-2 (+3.45%). Thus, both CF formulations remained substantially better than the aged base mud. Cake thickness changed from 2.10 to 2.20 mm in the base mud, from 1.70 to 1.75 mm in CF-1 and from 1.30 to 1.40 mm in CF-2. These small absolute changes indicate that the fibre-containing cakes remained relatively stable under the ageing condition used. The results demonstrate useful thermal retention at 65 °C, but they should not be interpreted as evidence of HPHT stability. Temperature, particle concentration and biomass chemistry can strongly influence drilling-mud behaviour, and higher-temperature and contaminated-mud tests are required before field deployment **[8]; [10].**

Table 9. Properties of the mud samples after ageing at 65 °C for 16 h.

Sample	pH	PV (cP)	AV (cP)	YP (lb/100 ft²)	10-s gel	10-min gel	Filtrate (mL)	Cake (mm)
Base Mud	9.10 ± 0.05	27.0 ± 1.0	38.0 ± 1.0	22.0 ± 1.0	8.0 ± 0.6	14.0 ± 1.0	24.0 ± 0.5	2.20 ± 0.10
CF-1	8.95 ± 0.05	30.0 ± 1.0	42.0 ± 1.0	24.0 ± 1.0	10.0 ± 1.0	17.0 ± 1.0	18.5 ± 0.5	1.75 ± 0.10
CF-2	8.80 ± 0.05	34.0 ± 1.0	47.0 ± 1.0	26.0 ± 1.0	12.0 ± 1.0	20.0 ± 1.0	15.0 ± 0.5	1.40 ± 0.10

Table 10 shows that ageing at 65 °C for 16 h increased the plastic viscosity (PV), apparent viscosity (AV) and yield point (YP) of all drilling-fluid formulations. PV, AV and YP increased from 24 to 27 cP, 31 to 38 cP and 14 to 22 lb/100 ft², respectively, for the base mud; from 27 to 30 cP, 35 to 42 cP and 16 to 24 lb/100 ft² for CF-1; and from 30 to 34 cP, 39 to 47 cP and 18 to 26 lb/100 ft² for CF-2. These increases correspond to PV, AV and YP changes of 12.50%, 22.58% and 57.14% for the base mud; 11.11%, 20.00% and 50.00% for CF-1; and 13.33%, 20.51% and 44.44% for CF-2, respectively. PV reflects the contribution of suspended-solids interactions and mechanical friction to flow resistance, while AV describes the overall viscosity at the specified measurement condition and YP indicates the extrapolated stress associated with

(This work is licensed under a Creative Commons Attribution 4.0 International License.)

International Journal of Engineering Research & Technology (IJERT)
ISSN: 2278-0181
Vol. 15 Issue 10 , October - 2026

initiating flow; consequently, increases in these parameters suggest that the mud systems became more viscous and developed greater resistance to flow after ageing **[11]; [19].** These changes may be associated with alterations in bentonite hydration, particle interactions and the structure of the suspended solids, although these mechanisms were not independently investigated in the present study. The results are consistent with established literature showing that drilling-fluid rheology depends on formulation, additive characteristics and ageing conditions **[19]**. Research on cellulose-based additives also demonstrates that lignocellulosic and polymeric materials can influence the rheological behaviour of water-based drilling fluids, although coconut fibre should not be considered equivalent to purified cellulose derivatives **[2].** Compared with studies involving more severe thermal conditions, the increase in rheological properties observed in this work indicates that the formulations responded differently under the relatively mild ageing conditions of 65 °C for 16 h; therefore, direct numerical comparisons with studies using different temperatures, additives and ageing durations should be made cautiously. Among the tested formulations, CF-2 maintained the highest aged PV, AV and YP values of 34 cP, 47 cP and 26 lb/100 ft², respectively, indicating the greatest rheological strength under the experimental conditions. In contrast, CF-1 exhibited the smallest relative increase in PV (11.11%), suggesting a comparatively lower change in this parameter during ageing. However, higher viscosity and yield point do not necessarily indicate superior drilling-fluid performance because excessive rheological resistance may increase pumping pressure and equivalent circulating density, whereas insufficient values may compromise cuttings transport and suspension **[11]; [19]**. Consequently, the suitability of CF-1 and CF-2 should be evaluated alongside their filtration volumes, filter-cake thicknesses and gel strengths. Because the present study did not include replicate-based statistical analysis or direct measurements of particle interactions, the observed differences should be interpreted as experimental trends rather than statistically significant effects. Overall, the findings demonstrate that thermal ageing increased the measured rheological properties of all three formulations, with CF-2 producing the highest absolute values and CF-1 exhibiting the smallest relative PV increase. Further evaluation of filtration control and other operational properties is necessary before identifying the most suitable formulation for drilling applications **[20].**

Table 10. Comparison of selected unaged and aged properties after ageing at 65 °C for 16h.

Sample	Unaged Mud			Aged mud (65 °C, 16 h)		
	PV (cP)	AV (cP)	YP (lb/100 ft²)	PV (cP)	AV (cP)	YP (lb/100 ft²)
Base Mud	24	31	14	27	38	22

(This work is licensed under a Creative Commons Attribution 4.0 International License.)

International Journal of Engineering Research & Technology (IJERT)
ISSN: 2278-0181
Vol. 15 Issue 10 , October - 2026

CF-1	27	35	16	30	42	24
CF-2	30	39	18	34	47	26

3.7 Effect of Coconut Fibre Loading

Increasing CF loading from 12.5 to 25.0 g per 250 mL produced a monotonic improvement in filtration control under the tested conditions. Filtrate loss decreased from 18.0 to 14.5 mL and cake thickness decreased from 1.70 to 1.30 mm, while PV increased from 27.0 to 30.0 cP and YP increased from 16.0 to 18.0 lb/100 ft². The response suggests that additional fibre increased the availability of bridging material in the filter-cake structure. However, the same loading increase also reduced density and increased gel strength, demonstrating the need to balance filtration improvement against the requirements of mud weight and rheological control.

Table 10. Percentage change in selected unaged mud properties relative to the base mud.

Property	CF-1 (5 g/100 mL)	CF-2 (10 g/100 mL)
Density	−23.48%	−25.22%
pH	−10.71%	−11.31%
PV	+12.50%	+25.00%
AV	+12.90%	+25.81%
YP	+14.29%	+28.57%
10-s gel	+33.33%	+66.67%
10-min gel	+30.00%	+60.00%
Filtrate loss	−20.00%	−35.56%
Cake thickness	−19.05%	−38.10%

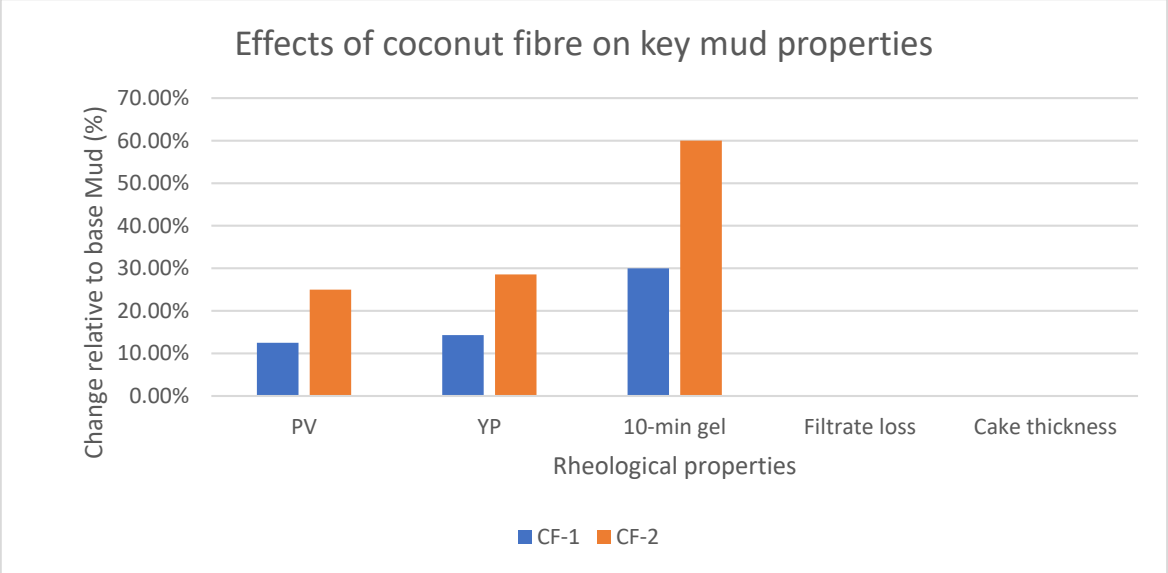


Figure 11. Effect of CF loading on selected key mud properties relative to the base mud.

(This work is licensed under a Creative Commons Attribution 4.0 International License.)

International Journal of Engineering Research & Technology (IJERT)
ISSN: 2278-0181
Vol. 15 Issue 10 , October - 2026

3.8 Comparative Performance Assessment

A single formulation cannot be declared universally optimal because the preferred mud depends on the required density, rheological window, filtration target and thermal conditions. Within this experiment, CF-2 was the strongest filtration-control formulation, giving the lowest filtrate loss (14.5 mL) and thinnest cake (1.30 mm). CF-1, however, showed slightly smaller changes in most properties after thermal ageing and produced a more moderate increase in PV, YP and gel strength. Therefore, CF-2 is best described as the strongest filtration performer among the tested formulations, whereas CF-1 provides a more conservative rheological and ageing profile. Neither should be treated as a field optimum without additional density adjustment and performance testing.

Table 11. Comparative performance summary of CF-modified muds.

Criterion	CF-1	CF-2	Interpretation
Filtrate loss	18.0 mL; −20.00%	14.5 mL; −35.56%	CF-2 better
Cake thickness	1.70 mm; −19.05%	1.30 mm; −38.10%	CF-2 better
PV	27.0 cP; +12.50%	30.0 cP; +25.00%	CF-1 more moderate
YP	16.0; +14.29%	18.0; +28.57%	CF-1 more moderate
10-min gel	13.0; +30.00%	16.0; +60.00%	CF-1 more moderate
Filtrate after ageing	18.5 mL	15.0 mL	CF-2 better
Cake after ageing	1.75 mm	1.40 mm	CF-2 better
Overall interpretation	Balanced response	Strongest filtration response	Selection depends on drilling objective

3.9 Mechanistic Interpretation

The observed behaviour can be interpreted in terms of the fibrous morphology and lignocellulosic chemistry of CF. The XRD result indicates a predominantly disordered structure, while FTIR confirms abundant hydroxyl and polysaccharide-related functional groups. The fibrous particles can provide a bridging framework across larger openings in the developing filter cake, while finer bentonite particles fill smaller voids. This combined structure can reduce cake permeability and therefore filtrate loss. Similar bridging and sealing behaviour has been proposed for coconut fibre and other biodegradable waste additives **[9]; [8]; [5].**

The progressive increase in PV, YP and gel strength with CF loading indicates that the fibre also participates in the suspended-particle network. Hydroxyl-rich surfaces may promote interaction with water and clay surfaces, but the present experiment did not directly measure adsorption, zeta potential, soluble ions or

(This work is licensed under a Creative Commons Attribution 4.0 International License.)

International Journal of Engineering Research & Technology (IJERT)
ISSN: 2278-0181
Vol. 15 Issue 10 , October - 2026

microstructure. Consequently, the proposed interactions remain mechanistic interpretations rather than directly demonstrated molecular mechanisms.

4. ENVIRONMENTAL AND PRACTICAL IMPLICATIONS

Converting coconut residue into a drilling-mud additive provides a potential route for agricultural-waste valorisation and the development of renewable mud materials. Recent reviews support the investigation of biodegradable and natural materials for rheology and filtration control in water-based muds **[5]; [6].** However, biological origin alone does not establish environmental superiority. Transport, drying and grinding energy, raw-material contamination, leaching behaviour, mud-waste handling and end-of-life disposal should be evaluated before claiming a complete environmental advantage. The present data also show an important practical constraint: CF markedly reduced mud density. Consequently, a CF-containing formulation would require density management if used in a well where a higher mud weight is required. The additive should therefore be considered a functional rheology/filtration modifier rather than a replacement for barite. Standardized fibre preparation and particle-size control will also be necessary because biomass properties can vary with source, maturity and processing history **[6].**

5. LIMITATIONS

The investigation was conducted under laboratory conditions using fresh-water bentonite mud and ageing at 65 °C for 16 h. The CF loadings were relatively high, and lower concentrations were not investigated. Salinity, calcium contamination, drilled solids, formation mineralogy, HPHT filtration, lubricity, shale inhibition and dynamic cuttings-transport performance were not evaluated. CF was characterised by XRD and FTIR, but elemental composition, detailed particle-size distribution, morphology, thermal decomposition behaviour and soluble-ion release were not measured. The XRD pattern was dominated by amorphous scattering, so automated candidate-phase matches were not accepted as evidence of crystalline phases. These limitations define the scope of the conclusions and identify the principal experiments required for further development.

6. CONCLUSIONS

This study evaluated coconut fibre (CF) as an agricultural-waste additive in a bentonite–barite water-based drilling mud, focusing on its physicochemical characteristics, rheological behaviour, filtration control and response to thermal ageing. X-ray diffraction (XRD) revealed a broad principal maximum at $2\theta = 21.36 \pm 0.06°$ without resolved sharp crystalline reflections, suggesting predominantly amorphous or poorly crystalline material, while Fourier-transform infrared spectroscopy (FTIR) identified hydroxyl, aliphatic C–H, aromatic and C–O/C–O–C functional groups consistent with the cellulose–lignin composition of lignocellulosic biomass **[16]; [21]** Incorporating coconut fibre reduced mud density from 11.50 ppg in the

(This work is licensed under a Creative Commons Attribution 4.0 International License.)

International Journal of Engineering Research & Technology (IJERT)
ISSN: 2278-0181
Vol. 15 Issue 10 , October - 2026

base mud to 8.80 and 8.60 ppg at loadings of 12.5 and 25.0 g, respectively, while pH decreased from 8.40 to 7.50 and 7.45. These changes demonstrate that the additive influenced the physical and chemical properties of the formulated mud, highlighting the need to monitor density and alkalinity when incorporating agricultural residues into water-based drilling fluids **[11].**

The addition of coconut fibre progressively increased plastic viscosity (PV), apparent viscosity (AV), yield point (YP) and gel strength, indicating changes in the flow behaviour and internal structure of the mud. At the higher loading of 25.0 g, PV, AV and YP increased by 25.00%, 25.81% and 28.57%, respectively, relative to the base mud. These changes are consistent with the established role of suspended particles and additive–clay interactions in controlling drilling-fluid rheology, although the specific mechanisms responsible for the observed changes require further investigation **[11]; [19].** Filtration performance also improved with coconut fibre incorporation: CF-1 reduced filtrate loss by 20.00% and filter-cake thickness by 19.05%, whereas CF-2 achieved reductions of 35.56% and 38.10%, respectively, relative to the base mud. These findings suggest that coconut fibre can contribute to filtration control, an important function in limiting excessive filtrate invasion and filter-cake development during drilling operations **[20]**. Following ageing at 65 °C for 16 h, both CF-containing formulations maintained lower filtrate loss than the aged base mud, indicating that their filtration-control performance was retained under the laboratory ageing conditions. Although CF-1 exhibited smaller proportional changes in some rheological properties, CF-2 maintained the strongest filtration performance among the formulations tested. Nevertheless, the substantial reduction in mud density and the increases in rheological parameters and gel strength indicate that filtration performance alone is insufficient to establish the overall suitability of an additive for field application. In conclusion, coconut fibre shows potential as a locally available agricultural-waste additive for improving the filtration control of bentonite–barite water-based drilling mud; however, further optimization is required to balance filtration performance, density, rheology, gel strength and operational requirements. These conclusions are limited to the formulations and laboratory conditions investigated, and additional testing is necessary before field-scale application can be recommended **[11]; [19]; [20]**

7. RECOMMENDATIONS FOR FUTURE WORK

I. Investigate lower CF concentrations and optimise particle size to identify a practical filtration/rheology balance.
II. Determine CF elemental composition and soluble-ion release using XRF or SEM–EDS and aqueous extraction tests.
III. Characterise particle morphology and size distribution by SEM and laser diffraction and evaluate thermal decomposition using TGA.
IV. Measure lubricity, shale inhibition, dynamic filtration and cuttings-transport performance.

(This work is licensed under a Creative Commons Attribution 4.0 International License.)

International Journal of Engineering Research & Technology (IJERT)
ISSN: 2278-0181
Vol. 15 Issue 10 , October - 2026

V. Assess leachability, biodegradability, toxicity, processing energy and life-cycle impacts before making field-scale environmental claims.

DECLARATIONS

Author contributions: Igoru Ufuoma Alex conceived the study, prepared the coconut fibre, formulated and tested the mud samples, analysed the experimental results, prepared the figures and tables, and wrote and revised the manuscript.

Funding: No external funding was reported for this study.

Conflict of interest: The author declares no conflict of interest.

Data availability: The numerical results used in this manuscript are presented in the tables and figures. Additional underlying laboratory records are available from the corresponding author on reasonable request.

Acknowledgements: The author acknowledges the laboratory facilities of the Department of Petroleum and Gas Engineering, Delta State University, Oleh Campus.

REFERENCES

[1] Mahmoud, H., Mohammed, A. A. A., Nasser, M. S., Hussein, I. A., & El-Naas, M. H. (2024). Green drilling fluid additives for a sustainable hole-cleaning performance: A comprehensive review. *Emergent Materials, 7*, 387–402. https://doi.org/10.1007/s42247-023-00524-w

[2] Khan, M. A., Li, M.-C., Lv, K., Sun, J., Liu, C., Liu, X., Shen, H., Dai, L., & Lalji, S. M. (2024). Cellulose derivatives as environmentally-friendly additives in water-based drilling fluids: A review. *Carbohydrate Polymers, 342*, 122355. https://doi.org/10.1016/j.carbpol.2024.122355

[3] Al-Rubaii, M., Al-Shargabi, M., & Al-Shehri, D. (2023). Hole cleaning during drilling oil and gas wells: A review for hole-cleaning chemistry and engineering parameters. Advances in Materials Science and Engineering, 2023, Article 6688500. https://doi.org/10.1155/2023/6688500

[4] Al-Ziyadi, H., & Verma, A. (2025). Smart additives for fluid loss control in water-based drilling fluid: A review of recent developments. Petroleum Research, 10(4), 882–893. https://doi.org/10.1016/j.ptlrs.2025.06.005

[5] Fato, D. A., & Rahmani, O. (2024). Enhancing drilling fluid properties using biodegradable waste additives: A comprehensive study on water- and oil-based systems. *Journal of Environmental Management, 370*, 123007. https://doi.org/10.1016/j.jenvman.2024.123007

[6] Wu, Y., You, F., & Hou, S. (2025). Application of natural materials containing carbohydrate polymers in rheological modification and fluid loss control of water-based drilling fluids: A review. Carbohydrate Polymers, 348, 122928. https://doi.org/10.1016/j.carbpol.2024.122928

[7] Rencoret, J., Ralph, J., Marques, G., Gutiérrez, A., Martínez, Á. T., & del Río, J. C. (2013). Structural characterization of lignin isolated from coconut (Cocos nucifera) coir fibers. Journal of Agricultural and Food Chemistry, 61(10), 2434–2445. https://doi.org/10.1021/jf304686x

[8] Gyanchandani, Y., Patni, H., Shukla, P., Chauhan, Y., Bajoria, A., Ramalingam, V., & Bera, A. (2025). Investigation on the effect of coconut husk biofiber powder on the rheological and filtration properties of water-based drilling fluid. *Geoenergy Science and Engineering, 244*, 213411. https://doi.org/10.1016/j.geoen.2024.213411

[9] Chowdhury, A. N., & Rashid, M. M. U. (2025). Experimental study of coconut fiber as a fluid loss control additive to prepare an eco-friendly drilling fluid. SCS: Engineering, 3, 468–473. https://doi.org/10.38032/scse.2025.3.128

[10] Oguamah, I., Igwilo, K., Oseh, J., & Udeagbara, S. (2026). Burnt coconut fibre as a sustainable additive for water-based drilling fluids: Rheological, filtration, and physicochemical evaluation. *Next Materials, 12*, 102253. https://doi.org/10.1016/j.nxmate.2026.102253

[11] Caenn, R., Darley, H. C. H., & Gray, G. R. (2017). Composition and properties of drilling and completion fluids (7th ed.). Gulf Professional Publishing. https://doi.org/10.1016/C2015-0-04159 4

[12] Moraes, F. P., Cordeiro, N. G. B., Bojorge, N., & Alhadeff, E. M. (2024). Coconut fibre for the synthesis of micro fibrillated cellulose: Thermal analysis experimental characterization. The Canadian Journal of Chemical Engineering, 102(10), 3405–3415. https://doi.org/10.1002/cjce.25270

[13] Chand, O., Chopra, L., Raju, N. N., Asthana, N., Malik, A., & Khan, A. A. (2024). Extraction of micro fibrous cellulose from coconut husk by using chlorine free process: Potential utilization application as a filter aid. Journal of Molecular Structure. https://doi.org/10.1016/j.molstruc.2024.139325

[14] Mohan, P., Mohd Yusof, N. S., Thomas, S., & Abd Rahman, N. M. M. (2024). Ultrasound-alkali-assisted isolation of cellulose from coconut shells. BioResources, 19(4), 7870–7885. https://bioresources.cnr.ncsu.edu/resources/ultrasound-alkali-assisted-isolation-of-cellulose-from-coconut-shells/

[15] Zugenmaier, P. (2021). Order in cellulosics: Historical review of crystal structure research on cellulose. Carbohydrate Polymers, 254, 117417. https://doi.org/10.1016/j.carbpol.2020.117417

[16] French, A. D. (2014). Idealized powder diffraction patterns for cellulose polymorphs. Cellulose, 21(2), 885–896. https://doi.org/10.1007/s10570-013-0030-4

[17] Socrates, G. (2001). Infrared and Raman characteristic group frequencies: Tables and charts (3rd ed.). John Wiley & Sons.

[18] American Petroleum Institute. (2026). *API Recommended Practice 13B-1: Testing water-based drilling fluids* (6th ed.). American Petroleum Institute.

[19] Agwu, O. E., Akpabio, J. U., Ekpenyong, M. E., Inyang, U. G., Asuquo, D. E., Eyoh, I. J., & Adeoye, O. S. (2021). A critical review of drilling mud rheological models. *Journal of Petroleum Science and Engineering, 203*, 108659. https://doi.org/10.1016/j.petrol.2021.108659

[20] American Petroleum Institute. (2023). *API Recommended Practice 13B-1: Recommended Practice for Field Testing Water-Based Drilling Fluids*. API. Confirm the edition and applicable errata against the standard used in your laboratory.

(This work is licensed under a Creative Commons Attribution 4.0 International License.)

International Journal of Engineering Research & Technology (IJERT)
ISSN: 2278-0181
Vol. 15 Issue 10 , October - 2026

[21] Poletto, M., Ornaghi, H. L., & Zattera, A. J. (2014). Native cellulose: Structure, characterization and thermal properties. *Materials, 7*(9), 6105–6119. https://doi.org/10.3390/ma7096105

(This work is licensed under a Creative Commons Attribution 4.0 International License.)